Air-Gap Transmission Lines for OEICs and MMICs Using Glass Substrates

J. Chuang, S. M. El-Ghazaly, D. K. Schroder, Y. H. Zhang , G. N. Maracas*, A. C. Reyes*

Department of Electrical Engineering, Center for Solid State Electronics Research,
Arizona State University, Tempe, AZ 85287-5706
*Motorola, Inc., MD: EL720, 2100 E. Elliot Rd., Tempe, AZ 85284

Abstract

This paper describes transmission-line structures for optoelectronic integrated circuits (OEICs) and monolithic microwave integrated circuits (MMICs) using glass processing assisted microbump bonding (GPAMBB). Two different configurations of air-gap transmission lines are fabricated using this interconnection technique. Because the field distributions are mainly in air, these structures have the advantages of low losses, and low dispersion. Theoretical and experimental results of both structures are presented in this paper. The attenuation of the two air-gap transmission lines and the conventional CPW are compared over the 2 GHz - 20 GHz range.

INTRODUCTION

This paper introduces two types of air-gap transmission lines, the air-gap microstrip line (AGML) and the air-gap coplanar waveguide (AGCPW) which are integrated with a semiconductor substrate using the glass processing assisted microbump bonding method (GPAMBB) to produce precise controlled air-gap height. Fig. 1 is a simplified cross-section view of the air-gap transmission lines and a coplanar waveguide (CPW). Air-gap transmission lines using GPAMBB enable several important advancements in OEICs and MMICs. For OEICs, the successful development in low-threshold current and high frequency operation of GaAs vertical-cavity surface-emitting lasers (VCSELs) has stimulated a great deal of research and development for the integration VCSELs arrays with microelectronics and micro-optics can be performed over an entire wafer [1]. This integration opens numerous challenges in optical interconnects to make a smooth optical signal transition from VCSELs into waveguides or free space. Low cost glass substrates are highly transparent over the 0.4 μm to 1.2 μm region of the optical spectrum which is an essential part to be used as a microlens substrate for most VCSELs integration.

Furthermore, recent rapid advances in MMICs development are also placing increasing demands on circuit interconnection techniques for which high frequency signal can be propagated through interconnection lines without sacrificing circuit performance. At present, the most common interconnection line structures in monolithic integrated circuit technology are the microstrip line and coplanar waveguide configurations. The geometric structure of these interconnects can change the propagating field distribution which has a large impact on the performance of the circuits, because losses and dispersion characteristics of the transmission lines over a semiconductor degrade the high frequency signal performance. Air-gap transmission lines have the propagating waves concentrated in air, which minimizes both losses and dispersion.

The performance of air gap interconnects for microwave transmission lines will be examined in this paper. Specifically, this paper will compare the frequency performance of AGML and AGCWP with conventional CPW.

THEORETICAL ANALYSIS AND DESIGN

Recently, transmission lines on semiconductor substrates have been investigated and considered as Schottky (metal-semiconductor) junctions or metal-insulator-metal junctions using solid state physics concepts [2,3]. Microwave loss analysis results confirm that high frequency performance of interconnects on semiconductor are affected by semiconductor surface conditions as well as the properties of bulk substrates. Obviously, the electromagnetic wave propagation characteristics of air-gap structures are considerably less affected by the properties of semiconductor substrates. The

0-7803-4603-6/97/$5.00 (c) IEEE

quasi-TEM mode propagation characteristics of both air-gap transmission lines are simulated using the SILVACO ATLAS semiconductor simulator. In this simulation, the continuity equation was not taken into account because most of the semiconductor surface is shielded by the ground plane for the air-gap configurations so the interactions between the electric field and the semiconductor electrons [4] are minimized. After the capacitances of both air gap structures are extracted from the Poisson solver, the effective dielectric constant and characteristic impedance can be obtained.

Both AGML and AGCPW structures are simulated under three different cases for comparison purpose. In case 1, a signal line is suspended in air without any cover material. Case 2 and 3, the signal lines are covered by glass (ε_r =2.25) and silicon (ε_r =12), respectively. The characteristics of AGML under these three cases are shown in Fig. 2 and 3. The characteristic impedance of this structure can be varied over a relatively wide range by controlling the structure geometry. The effective dielectric constant is very close to one when the signal line is covered by a glass substrate, which demonstrates the very low dispersion potential of this structure. For the AGCPW structure with fixed W = 100 μm and 2b = 240 μm, the properties of this configuration under these conditions are shown in Fig. 4 and 5. AGCPW structure has a higher characteristic impedance since the field lines are mostly in air and the a lower capacitance per unit length. The characteristic impedance can be reduced by controlling the ground gap spacing 2b.

FABRICATION

Fig. 6 illustrates a glass substrate bonded to a semiconductor substrate using the glass processing assisted microbump bonding (GPAMBB) method. The glass etching process starts by standard photolithography and wet chemical etching using hydrofluoric (HF) acid, several 100μm x 200μm glass microbumps with 15μm in height were patterned on the top surface of a thin (150 μm) glass slide. Following E-beam evaporation of 1 μm thickness Al metal for signal transmission lines on a glass substrate, the glass substrate is cut using a dicing saw to present the microbumps at the edge of the glass slide. After applying a small amount of UV curable epoxy onto a small portion of the semiconductor substrate surface, the microbumps covered by metal lines on the glass substrate are aligned to the signal launchers on the semiconductor substrate with a regular UV contact aligner. By taking advantage of the glass substrate optical transparency in the UV region, the bonding processing is simply accomplished by UV exposure. This approach produces a rigid bond between the glass substrate and the semiconductor substrate without any heat treatment. Furthermore, DC measurement results do not show any significant resistance increase (within the 10mΩ range) after the bonding process.

In this study all AGML, AGCPW, and CPW structures are constructed on a 500 μm thick 30Ω-cm resistivity silicon substrate. For the CPW structure, the signal line width (W) is 100 μm, line spacing (S) is 70 μm, and a 5000 μm line length is chosen. For both air gap structures, as shown in Fig. 6, the signal line width is 100 μm, the microbump height is 15 μm, the line length is 4400 μm, and microwave launcher for CASCADE probes is 500 μm which has 200 μm length contacted with glass microbumps. The only difference between both air gap configurations is the ground spacing (2b) of 240 μm in the AGCPW.

MEASUREMENT RESULTS

The transmission line characteristics were measured with an HP 8510A network analyzer with Cascade Microtech high frequency ground-signal-ground coplanar probes. A Short-Open-Load-Through (SOLT) calibration technique was performed and a 650 μm quartz plate was placed between the probe chuck and the substrate during the measurement. Fig. 7 shows the attenuation of the three different transmission lines. The CPW configuration has more than 5dB/cm loss compared to the two air-gap structures. The AGCPW structure also shows slightly higher insertion losses compared to the AGML structure. This is because the electric field interacts with the silicon substrate over the 240 μm ground spacing. The losses in air-gap configurations shown in Fig. 7 originate from two sources; from the air-gap transmission lines, and from two 500-μm-microwave launchers at the ends of the air-gap lines. The microwave launchers are realized in CPW configurations. In order to verify their effects, the s-parameters of a 1000-μm-long CPW were extracted from the measurement and taken into account in the following measurement. Figures 8 and 9 present a comparison between measured and simulated insertion loss of the air-gap transmission lines after extracting the effects of the microwave launchers. The measured and simulated

results agree within 0.4-dB for the AGML structure (Fig. 9). However, the measured and simulated results for AGCPW structure (Fig. 8) show 1-dB difference in the 6-9 GHz range. This difference may be due to neglecting the conductor losses in the simulation and tolerances in the air-gap transmission line dimensions due to variation in the fabrication process.

CONCLUSIONS

The quasi-TEM propagation characteristics of air gap interconnects were investigated in this paper. Both theoretical and experimental results prove that air-gap transmission lines can reduce both losses and dispersion effects compared to conventional CPW interconnects. Furthermore, the transmission characteristics of both air-gap configurations are significantly less affected by the semiconductor surface conditions and the bulk substrate properties. This can reduce the uncertainty of transmission-line modeling for monolithic circuit design. We have demonstrated the fabrication of air-gap interconnect lines using the glass microbump bonding method. The bonding costs are low and the process is simple. This bonding method has the potential of making a low cost solution for high frequency OEICs and MMICs technology.

Acknowledgment: The work has been supported in part by ARPA/ARO grants DAAH04-93-G-0248 and DAAH04-95-1-0252 and as well as equipment donations by Digital Electronics Corporation, Motorola, and Hewlet Packard.

REFERENCES

[1] R. Olbright, J. L. Jewell, R. P. Bryan, and W. S. Fu, "Micro-Optic and Microelectronic Integrated Packaging of Vertical Cavity Laser Arrays," Proc. SPIE., vol. 1851, pp. 97-105, 1993.

[2] A. C. Reyes, and S. M. El-Ghazaly, "Coplanar Waveguides and Microwave Inductors on Silicon Substrates," IEEE Trans. Microwave Theory Tech. vol. MTT43, pp.2016-2021, Sept. 1995.

[3] ZR. Hu, VF. Fusco, Y. Wu, HG. Gamble, BM. Armstrong and JAC. Stewart, "Contact Effects on HF of CPW High Resistivity Silicon Lines," IEEE MTT-S Digest, pp. 299-302, 1996.

[4] T. LaRocca, A. C. Reyes, and S. M. El-Ghazaly, "Analysis of Electromagnetic Wave Propagation on Coplanar Waveguides on Doped Semiconductor Substrates," International Microwave Symposium Digest, vol. 1, pp. 295-298, June 1996.

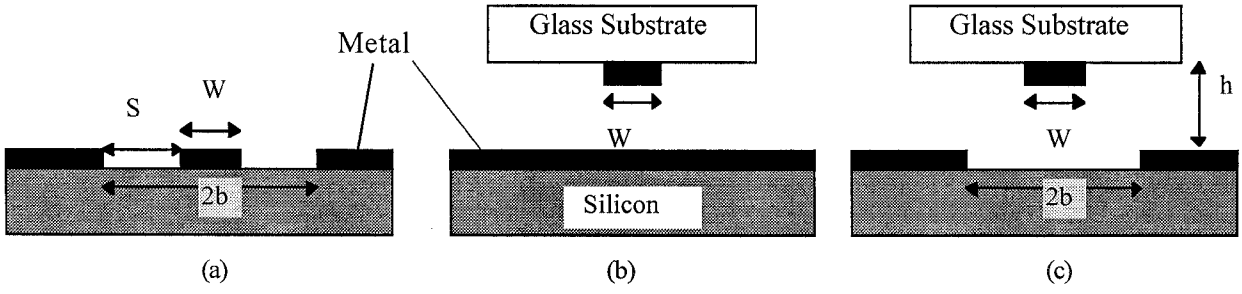

Figure 1: Cross section view of the (a) coplanar waveguide (CPW) (b) air-gap microstrip line (AGML) (c) air-gap coplanar waveguide (AGCPW) transmission lines configuration.

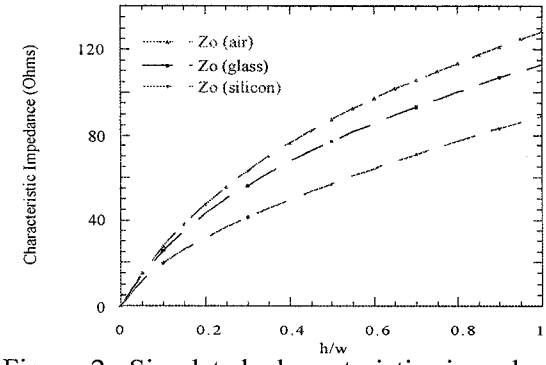

Figure 2: Simulated characteristic impedance of air gap microstrip line (AGML).

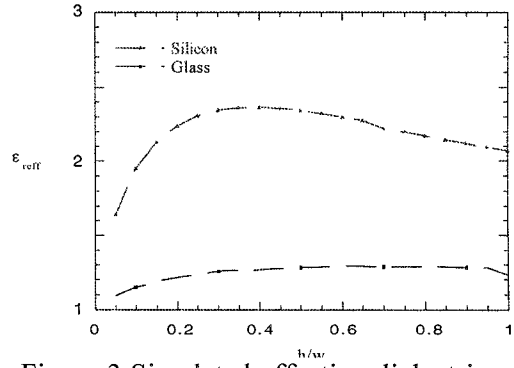

Figure 3:Simulated effective dielectric constant of air gap microstrip line.

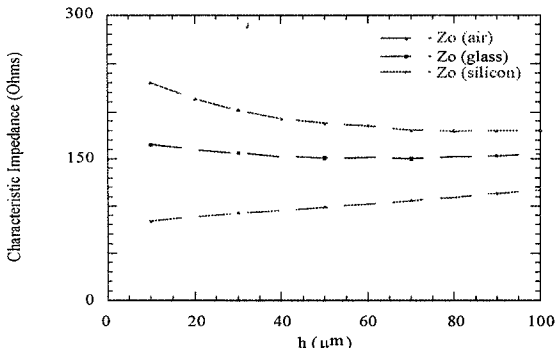

Figure 4: Simulated characteristic impedance of air-gap coplanar waveguide (AGCPW).

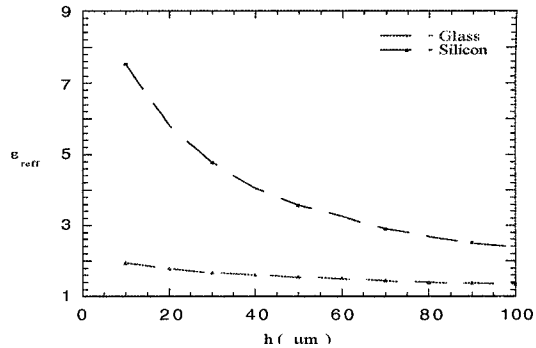

Figure 5: Simulated effective dielectric constant of air-gap coplanar waveguide.

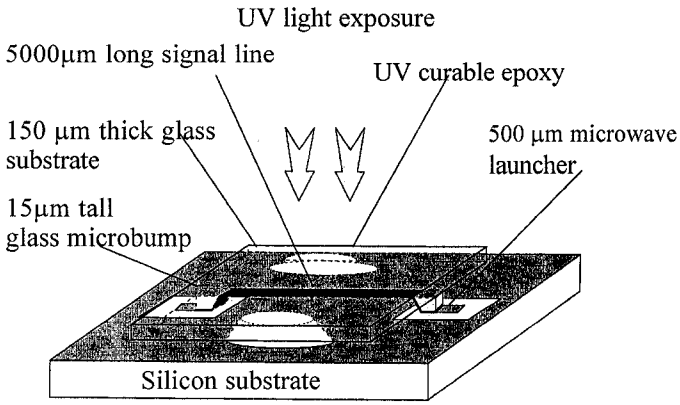

Figure 6: Simplified GPAMBB bonding process layout for glass substrate bonded to silicon substrate using UV curable epoxy for air-gap transmission lines.

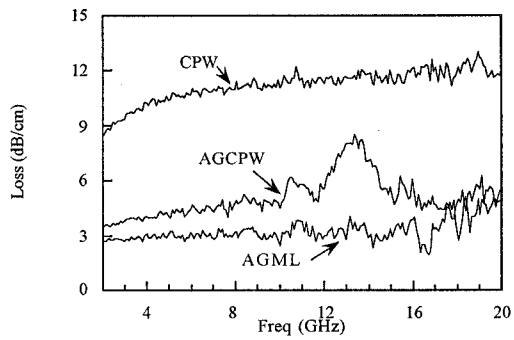

Figure 7: Measured losses of the three different transmission line configurations.

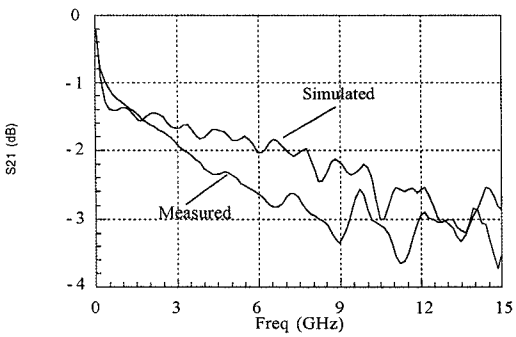

Figure 8: Measured and simulated insertion loss of a 5000-μm-long air-gap CPW (AGCPW).

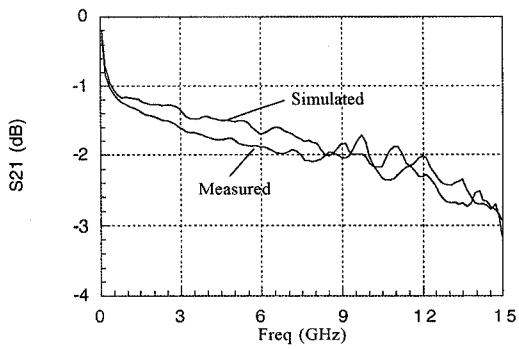

Figure 9: Measured and simulated insertion loss of a 5000-μm-long air-gap microstrip line (AGML).